

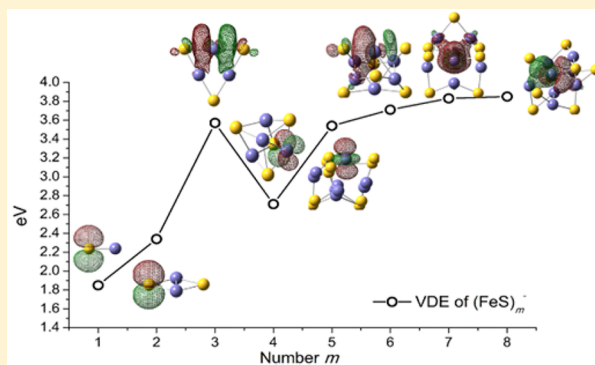
Photoelectron Spectroscopy and Density Functional Theory Studies of Iron Sulfur $(\text{FeS})_m^-$ ($m = 2-8$) Cluster Anions: Coexisting Multiple Spin States

Shi Yin¹ and Elliot R. Bernstein^{1*}

Department of Chemistry, NSF ERC for Extreme Ultraviolet Science and Technology, Colorado State University, Fort Collins, Colorado 80523, United States

Supporting Information

ABSTRACT: Iron sulfur cluster anions $(\text{FeS})_m^-$ ($m = 2-8$) are studied by photoelectron spectroscopy (PES) at 3.492 eV (355 nm) and 4.661 eV (266 nm) photon energies, and by density functional theory (DFT) calculations. The most probable structures and ground state spin multiplicities for $(\text{FeS})_m^-$ ($m = 2-8$) clusters are tentatively assigned through a comparison of their theoretical and experiment first vertical detachment energy (VDE) values. Many spin states lie within 0.5 eV of the ground spin state for the larger $(\text{FeS})_m^-$ ($m \geq 4$) clusters. Theoretical VDEs of these low lying spin states are in good agreement with the experimental VDE values. Therefore, multiple spin states of each of these iron sulfur cluster anions probably coexist under the current experimental conditions. Such available multiple spin states must be considered when evaluating the properties and behavior of these iron sulfur clusters in real chemical and biological systems. The experimental first VDEs of $(\text{FeS})_m^-$ ($m = 1-8$) clusters are observed to change with the cluster size (number m). The first VDE trends noted can be related to the different properties of the highest singly occupied molecular orbitals (NBO, HSOMOs) of each cluster anion. The changing nature of the NBO/HSOMO of these $(\text{FeS})_m^-$ ($m = 1-8$) clusters from a p orbital on S, to a d orbital on Fe, and to an Fe-Fe bonding orbital is probably responsible for the observed increasing trend for their first VDEs with respect to m .



INTRODUCTION

Iron sulfur clusters are ubiquitous and evolutionarily ancient prosthetic groups or cofactors that are required to sustain fundamental life processes. Interest in iron sulfur clusters is partially driven by their role as active centers of proteins,^{1,2} and their great significance in both industrial and biochemical catalysis.³⁻⁶ Iron sulfur clusters are prevalent in biological,⁷ as has been recognized for many decades. Owing to their remarkable structural plasticity and versatile chemical/electronic features, iron sulfur clusters participate in electron transfer, substrate binding/activation, iron/sulfur storage, regulation of gene expression, and enzyme activity. Understanding of the iron sulfur system grows with continuing and expanding investigations. These clusters play critical roles in the active sites of a wide variety of metalloproteins and metalloenzymes, which are involved in biological electron transfer processes,⁸ small molecule activation,⁹⁻¹¹ radical-based catalytic transformations,¹² DNA repair,¹³ and signal transduction.¹⁴ Therefore, investigations of iron-sulfur systems, ranging from bare Fe-S clusters to analogue complexes and proteins, are common throughout bioinorganic chemistry. Synthesis and characterization of iron sulfur clusters and complexes comprises a large subfield of organometallic chemistry.¹⁵ A number of studies have been performed on gas phase cationic,^{16,17}

neutral,^{18,19} and anionic²⁰⁻²⁷ iron sulfur clusters for investigation of their composition, stability, structure, and reactivity. Extensive theoretical efforts devoted to the structural evolution of electronic properties of iron-sulfur complexes have also appeared.²⁸⁻³²

To understand the mechanism(s) for iron sulfur cluster action, study of their electronic structure and properties is of course essential; such features as spin states of these clusters are significant and must be determined.^{33,34} Predicting the structure and the nature of bonding in stable organic or main group inorganic compounds are comparatively straightforward enterprises in the sense that the qualitative features of the electronic wave function of the ground state species are usually known. Transition metal chemistry stands in contrast to this situation, however. Many compounds involve metal centers, such as the iron sulfur clusters, with partially filled d shells and/or with one or several unpaired electrons. Therefore, predicting the orbital occupation pattern of a given stable compound is not always straightforward.

Received: August 2, 2017

Revised: September 8, 2017

Published: September 11, 2017

Computational and theoretical chemistry has a very important role to play in helping to predict and rationalize the nature of the electronic ground state of transition metal compounds.³⁵ Many strategies have been developed to understand the relationship between the remarkable structures of iron sulfur clusters (i.e., Fe_2S_2 , Fe_3S_4 , and Fe_4S_4) and their associated reactivity in biological systems;^{36–38} however, modeling iron sulfur proteins through ab initio methods becomes difficult because correct and reliable descriptions of iron sulfur bonding require extensive nondynamic correlation. Such calculations are very expensive and not predictively reliable for large systems.^{39,40} To probe the intrinsic properties of these systems, the exclusion of environmental effects is warranted¹⁶ and this approach can be rigorously achieved by gas phase experimental techniques. These results can then be directly and accurately compared to the calculated ones for the clusters of interest.²⁰

Photoelectron spectroscopy (PES) has been proven to be a successful approach for study of electronic and geometric structures of atomic and molecular clusters,⁴¹ as it combines size selectivity with spectral sensitivity. Moreover, in the calculation of photoelectron spectra properties of both ionic and neutral species must be explored. The predicted structure and properties (e.g., spectroscopic features) will of course be different for different spin and charge states. PES experimental results for cluster anions, such as iron sulfur cluster anions, are essential as tests for the performance of appropriate computational and theoretical methods. Electron binding energy of iron sulfur clusters obtained from theory can be compared with those obtained from experiment to justify the theoretical method. Theoretical results obtained by provably reliable calculations can then be employed to analyze further PES spectra and finally generate geometric structures and electronic properties for these iron sulfur clusters that are not directly observable experimentally.

This report presents a PES study of a series of iron sulfur cluster anions $(\text{FeS})_m^-$ ($m = 2–8$), employing a magnetic-bottle time-of-flight (MBTOF) photoelectron spectroscopy (PES) apparatus. The PES spectra of these cluster anions at 355 and 266 nm photon energies are reported, and the structural and electronic properties of these cluster anions are investigated by density functional theory (DFT). The most probable structures and ground state spin multiplicities of this small, neutral, and anionic cluster series are thereby tentatively assigned by comparing the theoretical first vertical detachment energies (VDEs) with their experiment values.

The relative energies of possible spin states and VDEs for these iron sulfur clusters are calculated and discussed. Values for the electron affinities (EA) of their neutral counterparts are presented and analyzed as well.

METHODS

Experimental Section. The MBTOF-PES experimental setup, consisting of a laser vaporization cluster/molecular source, an orthogonal acceleration/extraction reflectron time-of-flight (oaRETOF) mass spectrometer (MS), a mass gate, a momentum decelerator, and a MBTOF electron analyzer, employed in this work has been described previously in detail.^{42,43} Only a brief outline of the apparatus is given below. In this work, $(\text{FeS})_m^-$ clusters are generated by two different methods. One method is laser ablation of a mixed iron/sulfur target in the presence of a pure helium carrier gas (99.99%, General Air). The target is made by pressing a mixture of iron

(99.9%, Sigma-Aldrich) and sulfur (99.98%, Sigma-Aldrich) powders. Another method is laser ablation of a Fe foil target in the presence of a 1% H_2S in helium carrier gas. The mass spectra obtained from these two generation methods are given as Figure S1 and S2 in the Supporting Information. A 10 Hz, focused, 532 nm Nd^{3+} :YAG laser (Nd^{3+} :yttrium aluminum garnet) with ~ 3 mJ/pulse energy is used for the laser ablation. The expansion gas is pulsed into the vacuum by a supersonic nozzle (R. M. Jordan, Co.) with a backing pressure of typically 100 psi. Photoelectron spectra of iron sulfur cluster anions generated by the above two methods are found to be in good agreement with each other, which suggests the experimental temperature conditions of these two methods are similar. The PES spectra presented were collected when $(\text{FeS})_m^-$ clusters were generated by the first method described above: laser ablation of a mixed iron/sulfur powder target in the presence of a pure helium carrier gas.

Generated iron sulfur cluster anions enter the extraction region of the TOFMS/PES spectrometer through a 6 mm skimmer. Anions present in the expansion are extracted perpendicularly from the beam by pulsed voltage applied to the first extraction plate. The voltages on the extraction plates are -250 V (pulsed), 0 V, and $+750$ V, respectively. A liner for both anion and electron flight tube regions has the same voltage ($+750$ V) as the last extraction plate. Two sets of ion deflectors and one ion einzel lens are positioned downstream of the extraction plates. The anions are then analyzed by the oaRETOFMS. The photoelectron technique has the following energy conserving relationship: $h\nu = \text{EKE} + \text{EBE}$, in which $h\nu$ is the photon energy, EKE is the measured electron kinetic energy, and EBE is the electron binding energy. In order to obtain a photoelectron spectrum of the anions of interest, a three-grid mass gate is used for cluster and molecule anion mass selection. Following the mass gate, the mass selected ion beam enters a momentum decelerator. Both the pulse width and the pulse amplitude of the momentum decelerator can be optimized to achieve the best deceleration effect.

The mass selected and decelerated anions are exposed to different laser wavelengths (355 nm, 266 nm) at the photodetachment region. The photodetached electrons are energy analyzed by MBTOF-PES spectrometer. A cone shape permanent magnet is used for the high magnetic field (~ 700 G) generation at the anion beam/photo detachment laser interaction region. The permanent magnet is mounted on a vacuum motor controlled, linear translation stage (Physik Instrumente LPS-24), so that the position of the permanent magnet can be optimized for the best photoelectron spectrometer resolution. The 1 m electron flight tube is surrounded by a solenoid, which is covered with two layers of GIRON magnetic shielding metal. The electric current for the solenoid is about 0.8 A, which produces a magnetic field of ~ 10 gauss at the center of the flight tube. The photodetached electrons pass through the flight tube and are detected by a microchannel plate (MCP) detector. A resolution of $\sim 4\%$ (i.e., 40 meV/1.00 eV electron kinetic energy) for the overall MBTOF photoelectron spectroscopy apparatus can be achieved. Under the above operating conditions, PES resolution is no longer limited by Doppler broadening associated with the perpendicular motion of the ion beam with respect to the collection and flight path of the photodetached electrons: in other words, momentum deceleration for the ion cluster beam is efficacious. PES spectra are collected and calibrated at this resolution with known spectra of Cu^- .⁴⁴

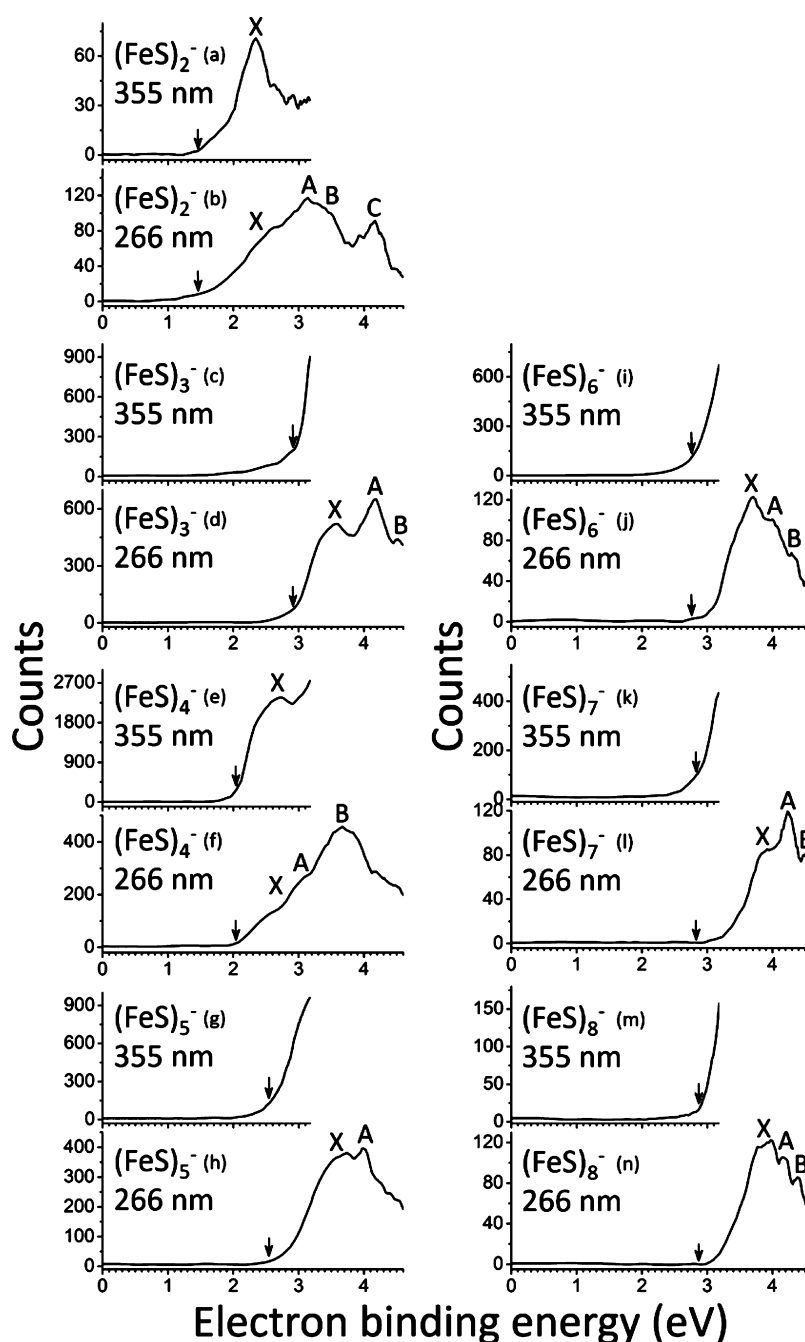


Figure 1. Photoelectron spectra of $(\text{FeS})_m^-$ ($m = 2-8$) cluster anions at 355 and 266 nm. X labels the ground state transition peak, and A, B, C label the first, second, and third low-lying transition peaks next to X, respectively.

Theoretical Section. All calculations are performed using the Gaussian 09 program package.⁴⁵ The structures of $(\text{FeS})_m^-$ ($m = 2-8$) clusters are optimized for different isomers and spin multiplicities using DFT without constraints. For each cluster, different initial structures are employed as input in the optimization procedure. There are many possible structures, especially for the larger clusters. Unfortunately, we are not able to calculate all possibilities. We try our best to search the global minimum structure for each cluster. For example, the linear and planar structures of $(\text{FeS})_8^-$ cluster are found to have higher relative energy than the cage structures, and 12 different initial cage structures were considered to find its global minimum structure. The geometry of each cluster shown in the following section is the lowest relative energy one among all possible

structures we considered. For each structure, spin multiplicities are scanned from low to high. All relative energies are zero point energy corrected. Vibrational frequency calculations are further performed to confirm global minima, which have zero imaginary frequency. The Perdew–Wang⁴⁶ correlation (BPW91) functional, combined with the triple- ζ valence plus polarization (TZVP) basis set,⁴⁷ which are proved to have good performance in previous studies of iron sulfur clusters,^{19,42} are employed to explore description of these clusters. Although the basis set TZVP is widely and successfully employed in theoretical studies of many metal containing anion clusters,⁴⁸⁻⁵¹ accurate and reliable theoretical DFT or ab initio calculations involving anions are thought to require the utilization of basis sets with diffuse functions. Therefore, basis

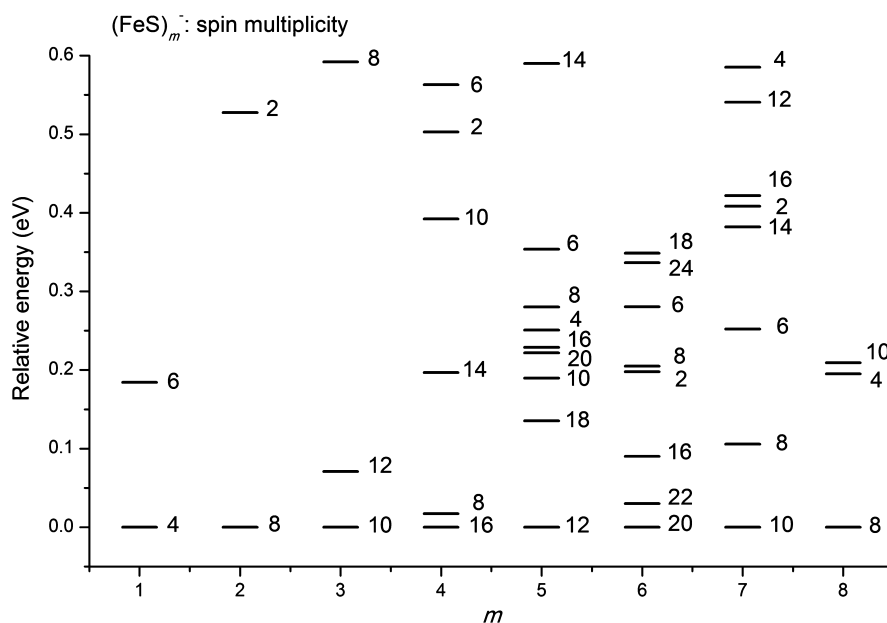


Figure 2. DFT calculated relative energies of different spin multiplicities of $(\text{FeS})_m^-$ ($m = 1-8$) cluster anions. The results for FeS^- are taken from ref 42.

sets with diffuse functions (e.g., 6-311+G(d)⁵²⁻⁵⁴ and aug-cc-PV5Z⁵⁵) are also selected in conjunction with the BPW91 functional for comparison with results obtained with the TZVP basis set, in order to determine if the TZVP basis set is sufficient to explore the description of iron sulfur anion clusters studied in this work. Calculated results for the relative energies (ΔE s) and first VDEs of the $(\text{FeS})_4^-$ clusters with different spin multiplicities do not depend on the chosen different basis sets (TZVP, 6-311+G(d), or aug-cc-PV5Z) (see Table 2 for details), and thereby are not significantly dependent on diffuse functions in this instance. These comparisons suggest that performance of the TZVP basis set is as good as that of basis sets containing diffuse functions, so the basis set TZVP is adopted in this work. The optimized anion geometries are used for the further calculations of the photoelectron spectra using time-dependent density functional theory (TDDFT)⁵⁶ also at BPW91/TZVP level. All calculations are treated in a spin-unrestricted manner. In this approach, for each spin state $(\text{FeS})_m^-$ anions, the first vertical detachment energy (VDE = $E_{\text{neutral at optimized anion geometry}} - E_{\text{optimized anion geometry}}$) is calculated as the lowest transition from the spin state (M) of the anion into the final lowest spin state ($M + 1$ or $M - 1$) of the neutral $(\text{FeS})_m$ species at the geometry optimized for the anion. Vertical excitation energies of the neutral species are added to the first VDE to obtain the second and higher VDEs of these $(\text{FeS})_m^-$ anion clusters. The outer valence Green function method (OVGF/TZVP)⁵⁷ is also used to calculate the second and higher VDEs. Calculated VDEs for each spin state of each $(\text{FeS})_m^-$ ($m = 2-8$) cluster are compared with experimental results.

A natural bond orbital (NBO) analysis is an often employed orbital localization and population analysis method. Within this method, natural atomic orbitals (NAOs), determined for the particular species under consideration, are evaluated and employed: NAOs are the effective orbitals of an atom in the particular molecular environment (rather than for isolated atoms). NAOs are also the maximum occupancy orbitals. Information obtained from an NBO analysis, such as partial

charges and HOMO–LUMO orbitals, is reported to explain, for example, a number of experimental phenomena of gas phase 1-butyl-3-methylimidazolium chloride ion pairs.⁵⁸ The NBO calculations in this work are performed using the NBO 3.1 program as implemented in the Gaussian 09 package.

RESULTS AND DISCUSSION

Photoelectron Spectra of $(\text{FeS})_m^-$ ($m = 2-8$). The obtained PES spectra for $(\text{FeS})_m^-$ ($m = 2-8$) clusters at different photon energies (355 and 266 nm) are shown in Figure 1. Photodetachment transitions occur between the ground state of an anion and the ground and excited states of its neutral counterpart, at the structure of the anion. The profile of the transition is governed by the Franck–Condon overlap between the two species, the anion and the neutral. The electron binding energy (EBE) value at the intensity maximum in the Franck–Condon profile is the vertical detachment energy (VDE). The first VDE, proving important in establishing a cluster's electronic and geometric structure, is derived from the energy of the first peak maxima in the photoelectron spectra. Broad peaks containing no reproducible fine structure are observed in most of the spectra of $(\text{FeS})_m^-$ ($m = 2-8$) clusters as displayed in the Figure 1, probably due to hot band related features for vibrations and spin states, effects of vibrational anharmonicity, and geometry differences between anions and neutrals.

The measured first VDE of $(\text{FeS})_2^-$ is 2.34 eV, clearly displayed in its 355 nm spectrum (Figure 1a). This result is consistent with the previously reported value (2.39 eV).²¹ In the spectrum of $(\text{FeS})_2^-$ at 266 nm (Figure 1b), broad peaks are observed for higher transitions as A, B, and C features (3.13, 3.46, and 4.17 eV).

For $(\text{FeS})_3^-$, three transitions are observed at EBE = 3.57, 4.17, and 4.51 eV in its 266 nm spectrum (Figure 1d). In the Figure 1c, only the start of the first peak is observed at low photon energy (355 nm, 3.49 eV), but a more accurate adiabatic electron affinity ($\text{EA} = E_{\text{optimized neutral}} - E_{\text{optimized anion}}$) for ground state $(\text{FeS})_3$ neutral cluster can be obtained (2.9

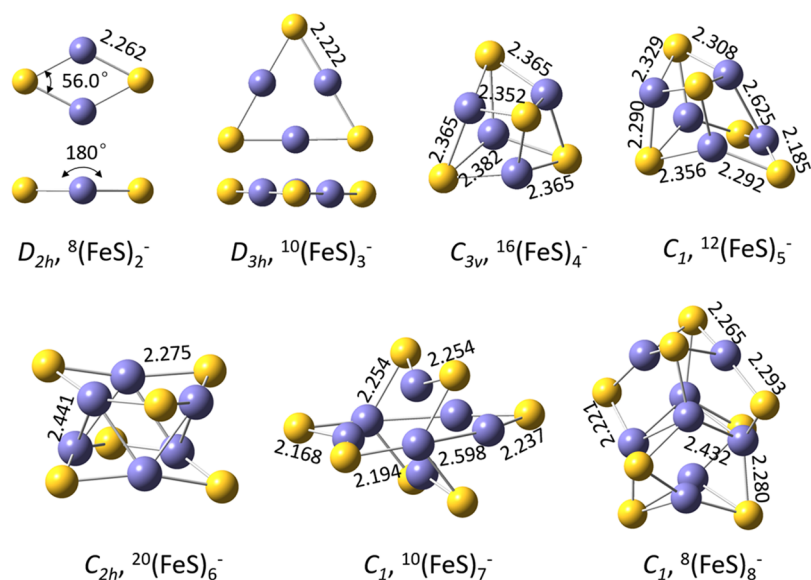


Figure 3. DFT optimized structures of $(\text{FeS})_m^-$ ($m = 2-8$) at the BPW91/TZVP level. Only the lowest relative energy spin state (shown in Figure 2) geometry of each cluster is displayed in this figure. Geometries of other spin states for each cluster are generally similar to the one shown but with slightly different bond lengths and angles. Bond lengths (in angstroms), bond angles (degrees), point group symmetry, and spin multiplicity $M^M(\text{FeS})_m^-$ are indicated on the structures.

eV), since the low kinetic energy electrons are generated from the near threshold photodetachment. To assign the experimental EA, the slope of the first onset is linearly extrapolated to the baseline of signal. The values of EA are indicated by a downward pointing arrow in the figure.

The first VDE of $(\text{FeS})_4^-$ is measured to be 2.71 eV at both 355 nm (Figure 1e) and 266 nm, and two higher transitions are observed at EBE = 3.09 and 3.69 eV in Figure 1f.

The $(\text{FeS})_5^-$, whose 266 nm spectrum is shown in Figure 1h, exhibits two broad transitions at EBE = 3.54 and 4.00 eV.

The spectra of $(\text{FeS})_6^-$, $(\text{FeS})_7^-$, and $(\text{FeS})_8^-$ show similar intensity patterns (Figure 1i–n). Their first VDEs are very close at 3.71, 3.83, and 3.85 eV, respectively. In each case, two higher transitions are observed in the range between 4.0 and 4.5 eV.

DFT Calculations for $(\text{FeS})_m^-$ ($m = 2-8$). The magnetic (spin) properties of iron sulfur clusters stand as their most fundamental characteristic and thereby provide an indispensable and essential means for their characterization. Therefore, spin-dependent delocalization for iron sulfur clusters, depicting ferromagnetic and antiferromagnetic spin alignments, is one of the most interesting, essential, and challenging topics for iron sulfur cluster studies.^{31,59,60} Here, the relative energies for each cluster with different spin multiplicities ($M = 2S + 1$) from low to high are investigated at the BPW91/TZVP level. Broken-symmetry³¹ is employed for low spin calculations (see details in the Supporting Information). Spin states of $(\text{FeS})_m^-$ ($m = 1-8$) clusters, whose relative energy differences (ΔE) are less than 0.6 eV, are summarized and displayed in Figure 2. The optimized structures of the lowest relative energy spin state clusters $(\text{FeS})_m^-$ ($m = 2-8$) and are shown in Figure 3. All of the optimized geometries shown in Figure 3 (in Cartesian coordinates), their total energies, and the $\langle S^2 \rangle$ values are given in the Supporting Information. Interestingly, geometries of other spin states for each cluster are generally similar to the one shown, but with slightly different bond lengths and angles. As shown in Figure 2, just two or three stable electronic states ($\Delta E < 0.6$ eV) are obtained for $(\text{FeS})_{1-3}^-$: the lowest energy

electronic state of $(\text{FeS})_2^-$ has $M = 8$ and second lowest energy state ($M = 2$) is 0.53 eV higher in energy. The larger clusters, $(\text{FeS})_{4-7}^-$, have multiple spin states close ($\Delta E < 0.6$ eV); for example, eight spin states are calculated within this energy range and the energies of the two lowest energy spin states $M = 20$ and $M = 22$ are very close (0.03 eV) for the $(\text{FeS})_6^-$ cluster anion. Three electronic states, $M = 8$, $M = 4$, and $M = 10$, are found at less than 0.2 eV energy difference for $(\text{FeS})_8^-$. The relative energies of the high spin states for $(\text{FeS})_8^-$ cluster are high; for example, the energy of electronic states $M = 20$ and $M = 22$ are 0.63 and 0.72 eV higher than that of its lowest energy electronic state ($M = 8$). $M = 20$ and $M = 22$ are not listed in Figure 2 because they are out of the range of this plot. Relative energies of different spin multiplicity for this cluster anion are given in Figure S3 of the Supporting Information.

To judge and assign the ground state spin multiplicity for these iron sulfur cluster anions, their theoretical first VDEs are compared with their respective experimental values.⁴² The calculated first VDEs of different spin state of these clusters obtained at the BPW91/TZVP level are summarized in Table 1. The experimental first VDE of $(\text{FeS})_2^-$ is 2.34 eV. The calculated first VDEs of $(\text{FeS})_2^-$ are 2.04 and 1.88 eV for $M = 8$ and $M = 2$ states, respectively. This comparison suggests the spin multiplicity of ground state $(\text{FeS})_2^-$ is an octet, which is in agreement with previous theoretical studies.^{29,61,62} The lowest energy electronic state of $(\text{FeS})_3^-$ has $M = 10$, and its calculated first VDE is 3.24 eV, 0.26 eV higher than the $M = 12$ state calculated value for $(\text{FeS})_3^-$. Since the experimental first VDE of this anion is 3.57 eV (Table 1), the ground state $(\text{FeS})_3^-$ is assigned to be $M = 10$. For $(\text{FeS})_4^-$, VDEs of five spin states are calculated. The calculated VDE of its lowest energy spin state ($M = 16$) is 2.87 eV and agrees well with the experimental value for $(\text{FeS})_4^-$ of 2.71 eV. Nonetheless, the calculated VDE of spin state $M = 14$ (2.76 eV) of $(\text{FeS})_4^-$ is in better agreement with the experimental value, although the energy of spin state $M = 14$ is about 0.2 eV higher than that of spin state $M = 16$. The calculated VDEs of other three spin states $M = 2, 8$, and 10 are 2.29, 2.20, and 1.83 eV, respectively, which are much lower

Table 1. First Calculated VDEs (in eV) for $(\text{FeS})_m^-$ ($m = 2-8$) at the BPW91/TZVP Level, as Well as the Experimental Results for Comparison^a

cluster	spin multiplicity	VDE (eV)	
		calculated	experimental
$(\text{FeS})_2^-$	8	2.04	2.34
	2	1.88	
$(\text{FeS})_3^-$	10	3.24	3.57
	12	2.98	
$(\text{FeS})_4^-$	16	2.87	2.71
	8	2.20	
	14	2.76	
	10	1.83	
$(\text{FeS})_5^-$	2	2.29	3.54
	12	3.08	
	18	3.13	
	10	3.06	
	20	3.26	
	16	3.02	
	4	3.04	
	8	2.56	
$(\text{FeS})_6^-$	6	2.86	3.71
	20	3.06	
	22	3.08	
	16	4.33	
	2	4.47	
	8	6.03	
	6	3.45	
	24	3.27	
$(\text{FeS})_7^-$	18	2.85	3.83
	10	3.50	
	8	3.59	
	6	3.63	
	14	3.84	
	2	3.73	
$(\text{FeS})_8^-$	16	3.47	3.85
	8	4.10	
	4	3.68	
	10	4.64	

^aDifferent spin multiplicities of each cluster are displayed in order of their relative energy low to high from top to bottom (see details in Figure 2).

than the experimental value 2.71 eV of $(\text{FeS})_4^-$. Considering both calculated relative energy and first VDE of spin states $M = 14$ and 16 , the ground state $(\text{FeS})_4^-$ cluster is tentatively

assigned to be $M = 16$: the spin state $M = 14$ very possibly is also present under the reported experimental conditions. The calculated first VDE value difference between spin states $M = 14$ and 16 of $(\text{FeS})_4^-$ cluster is only 0.11 eV, and their relative energy difference is also small (~ 0.2 eV). Because these differences are very close to the accuracy limit of DFT calculations, the above assignments should be considered tentative based solely on the BPW91/TZVP level of theory.

In order to generate a more secure assignment, different reasonable functionals (B3LYP,^{63,64} B3PW91,^{65,66} and APFD⁶⁷) and basis sets (6-311+G(d)⁵²⁻⁵⁴) are employed to calculate the relative energy and the first VDE of the $(\text{FeS})_4^-$ cluster with different spin multiplicities. The large basis set (LBS) aug-cc-PV5Z⁵⁵ for sulfur atoms and TZVP for iron atoms, are also employed and tested; the results of these studies are presented in Table 2. The relative energies of spin state $M = 16$ obtained with different functionals and basis sets are similar and near zero (less than 0.04 eV), and their calculated first VDEs are within 0.26 eV of each other using functionals B3PW91 and B3LYP with any of the above basis sets. These calculated results are in good agreement with the experimental value. Calculated VDEs obtained with the APFD functional are, on the other hand, much higher (~ 1 eV higher) than the experimental value. For the spin state $M = 14$, the calculated first VDEs are in range of 2.76–2.96 eV for all basis sets and functionals (excluding the APFD functional results), which agrees with the experiment value 2.71 eV very well. As the comparison and evaluation with different calculation methods are consistent, the assignment of $(\text{FeS})_4^-$ cluster at BPW91/TZVP level is apparently still reasonable, so the method BPW91/TZVP is selected to study other clusters, considering both the calculation accuracy and cost. Nonetheless, the relative energies of the different spin states are found to be different employing different functionals and basis sets for the calculations. For example, the lowest energy electronic state of $(\text{FeS})_4^-$ is found to be $M = 16$ at the BPW91/TZVP, B3LYP/TZVP, B3PW91/6-311+G(d), APFD/TZVP, and APFD/6-311+G(d) levels, to be $M = 8$ at BPW91/6-311+G(d) and BPW91/LBS levels, and to be $M = 2$ at B3LYP/6-311+G(d) level. This observation using B3LYP and B3PW91 functionals in conjugation with 6-311+G(d) basis set is in good agreement with published energy and spin state theoretical studies of iron sulfur clusters.⁶¹ Therefore, calculating the relative energy to determine the spin multiplicity of ground state of a cluster anion employing only one specific calculation method may be not cautious enough, especially for transition metal containing cluster anions for which the

Table 2. Calculated Relative Energy (ΔE) and the First VDE of $(\text{FeS})_4^-$ Cluster with Different Spin Multiplicity, Employing Different Functionals and Basis Sets for Comparison^a

methods	ΔE (eV)					VDE (eV)				
	$M = 16$	$M = 8$	$M = 14$	$M = 10$	$M = 2$	$M = 16$	$M = 8$	$M = 14$	$M = 10$	$M = 2$
BPW91/TZVP	0.00	0.02	0.20	0.39	0.50	2.87	2.20	2.76	1.83	2.29
BPW91/6-311+G(d)	0.01	0.00	0.19	0.33	0.46	3.04	2.42	2.94	2.04	2.51
BPW91/LBS	0.04	0.00	0.22	0.31	0.43	2.93	2.27	2.82	1.93	2.41
APFD/TZVP	0.00	0.67	0.42	0.78	1.10	3.74	5.16	3.69	3.79	5.51
B3LYP/TZVP	0.00	2.59	1.02	0.41	0.05	2.78	1.15	2.80	5.16	3.33
B3PW91/6-311+G(d)	0.00	2.72	1.09	0.57	1.12	2.86	1.52	2.89	4.79	2.71
B3LYP/6-311+G(d)	0.02	2.55	1.01	3.14	0.00	2.85	3.94	2.96	0.07	3.50
APFD/6-311+G(d)	0.00	4.51	0.42	2.92	3.16	3.85	2.53	3.87	2.32	3.45

^aThe experimental first VDE of $(\text{FeS})_4^-$ is 2.71 eV.

unpaired d electrons and high spin states are important and necessary to be considered. Employing various calculation methods for comparison and comparing calculation results with experimental values, such as the first VDE from PES results, are required to obtain a more secure, reliable, and believable assignment.

Following the above assignment procedures employed for the $(\text{FeS})_4^-$ cluster, the remaining larger clusters can be readily addressed. The spin multiplicity for the ground state of a cluster anion is assigned mainly based on agreement of the first calculated VDEs for the different spin multiplicities compared to the experimental values. ΔE values of different spin states under consideration are also evaluated and employed to generate the assignment for the larger clusters $(\text{FeS})_{5-8}^-$. These tentative assignments are obtained based on the calculation and experiment results displayed in Figures 1 and 2 and Table 1.

The ground state $(\text{FeS})_5^-$ cluster is assigned to be $M = 20$, and the spin states $M = 12, 18, 10, 16$, and 4 are likely populated under the present experimental conditions. The ground state $(\text{FeS})_6^-$ cluster is assigned to be $M = 6$, and spin states $M = 20, 22$, and 24 are probably populated in the experimental beam. The ground state $(\text{FeS})_7^-$ cluster is assigned to be $M = 14$, and the spin states $M = 10, 8, 6, 2$, and 16 are probably populated experimentally. The ground state $(\text{FeS})_8^-$ cluster is assigned to be $M = 4$, and the spin state $M = 8$ is probably populated as well. Calculated first VDEs for the above assigned ground states of $(\text{FeS})_m^-$ ($m = 2-8$) clusters are in good agreement with experimental first VDE values. Energy differences between calculated and experimental values are less than ~ 0.3 eV (Table 1), which is to be expected considering the accuracy limit of DFT calculations in general and the fact that calculated VDEs involve two species, an anionic and a neutral iron sulfur cluster.

The relative populations of these coexisting multiple spin states of the large iron sulfur $(\text{FeS})_{4-8}^-$ cluster anions can be generated either thermodynamically (through ΔE) or kinetically (through transition state barriers). The spin states $M = 20$ and 22 of $(\text{FeS})_6^-$ cluster are selected as a study example for this issue due to their low relative energy, small energy difference (0.035 eV), and similar calculated first VDE values. An ~ 0.12 eV energy barrier is obtained for transition from spin state $M = 20$ to $M = 22$ at the BPW91/TZVP calculation level, as shown in Figure 4. This calculated barrier suggests that transitions between different coexisting spin states may not be a barrierless process and that the apparent spin distribution suggested by the calculations can be related to both kinetic and thermodynamic causes.

Another issue for interconversion of spin multiplicity states for iron sulfur clusters is the effect of spin-orbit coupling (SOC). In order to have a general idea of the SOC effect, SOC corrected relative energies and the first VDEs calculations are performed for selected spin multiplicity $(\text{FeS})_{1,2}^-$ clusters using the MOLPRO program;⁶⁸ their results are shown in Table S1 and S2 of the Supporting Information. The SOC corrections are insignificant for the calculations of relative energies of the spin states and the first VDE of $(\text{FeS})_{1,2}^-$ clusters: details are given in the Supporting Information. Spin-orbit coupling may be important for larger clusters, however, which present a symmetrical environment for iron centers.⁶⁹ Therefore, the role of spin-orbit coupling may become more important for consideration of the relative populations of these coexisting multiple spin states, especially for the larger, more symmetric

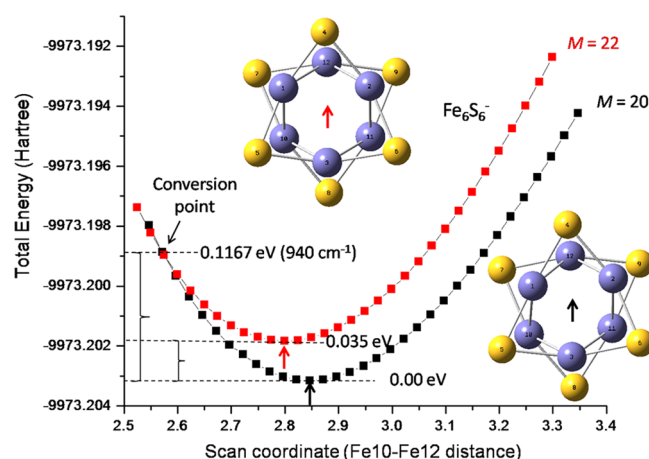


Figure 4. Spin conversion barrier observed from spin state $M = 20$ to $M = 22$ of $(\text{FeS})_6^-$ cluster, at the BPW91/TZVP calculation level.

iron sulfur cluster anions with spin multiplicity states that are nearly degenerate in energy (~ 0.1 eV). The relative energies of these spin states, especially in instances of near degeneracy, may be influenced by spin orbit interactions.

The EBE values after the first VDEs of these $(\text{FeS})_{2-8}^-$ clusters are calculated for their selected spin states employing both TDDFT at BPW91/TZVP level and OVGf/TZVP methods. Calculated results are summarized in Table 3 and compared with experimentally measured values. For $(\text{FeS})_{3,5-8}^-$ clusters, the EBEs calculated with TDBPW91/TZVP and OVGf/TZVP levels are found to agree well with each other. The TDBPW91/TZVP level of theory is more accurate for $(\text{FeS})_{2,4}^-$ clusters. Therefore, TDBPW91/TZVP is suggested for the higher transition energy theoretical studies for these

Table 3. Calculated Following EBE Values after the First VDE of $(\text{FeS})_{2-8}^-$ Clusters for Their Selected Spin States Employing TDDFT at BPW91/TZVP Level and OVGf/TZVP Methods

cluster	observed feature	experimental VDEs (eV)	calculated VDEs	
			TDDFT	OVGF
$(\text{FeS})_2^-$	X	2.34	2.04 ($M = 8$)	
	A	3.13	2.64	2.53
	B	3.46	2.94	3.13
	C	4.17	3.83	5.14
$(\text{FeS})_3^-$	X	3.57	3.24 ($M = 10$)	
	A	4.17	3.85	3.91
	B	4.51	4.25	4.11
$(\text{FeS})_4^-$	X	2.71	2.87 ($M = 16$)	
	A	3.09	3.43	3.06
$(\text{FeS})_5^-$	B	3.69	3.78	4.67
	X	3.54	3.08 ($M = 12$)	
$(\text{FeS})_5^-$	A	4.00	3.38	3.46
	X	3.71	3.06 ($M = 20$)	
$(\text{FeS})_6^-$	A	4.01	3.33	3.36
	B	4.34	3.67	3.64
	X	3.83	3.50 ($M = 10$)	
$(\text{FeS})_7^-$	A	4.24	3.63	3.67
	B	4.49	3.86	3.84
	X	3.85	4.10 ($M = 8$)	
$(\text{FeS})_8^-$	A	4.19	4.27	4.41
	B	4.39	4.33	4.60

iron sulfur clusters, as well. EAs for each ground state $(\text{FeS})_{2-8}$ neutral cluster, assigned through the above results, are calculated and summarized in Table 4. Neutral cluster

Table 4. Calculated Adiabatic Electron Affinity (EA) of Ground State $(\text{FeS})_m$ ($m = 2-8$) at the BPW91/TZVP Level, as Well as Their Experimental Results for Comparison

cluster	spin multiplicity	EA (eV)	
		calculated	experimental
$(\text{FeS})_2$	9	1.79	1.5
$(\text{FeS})_3$	11	3.15	2.9
$(\text{FeS})_4$	17	2.61	2.1
$(\text{FeS})_5$	19	2.95	2.6
$(\text{FeS})_6$	7	2.92	2.8
$(\text{FeS})_7$	13	3.48	2.8
$(\text{FeS})_8$	3	3.48	2.9

experimental EAs are also listed for comparison. Note that the obtained experimental EAs of these iron sulfur clusters are possibly affected by their anion vibrational hot bands due to their high-temperature generation conditions (~ 3 mJ/pulse ablation laser energy) and potential transition state barriers. Thus, their experimental EAs are possibly underestimated in this work.

Size-Dependent EA and VDE of $(\text{FeS})_m^-$ ($m = 1-8$) Clusters. Size specific iron sulfur clusters, such as $(\text{FeS})_2$ and $(\text{FeS})_4$, play an important role in activating enzymes and proteins, for which such iron sulfur clusters are the putative active centers. Investigation of the size-dependent EA and VDE changes for these iron sulfur clusters can provide useful information for understanding their size specific activity properties. Figure 5 plots the trends of experimental first

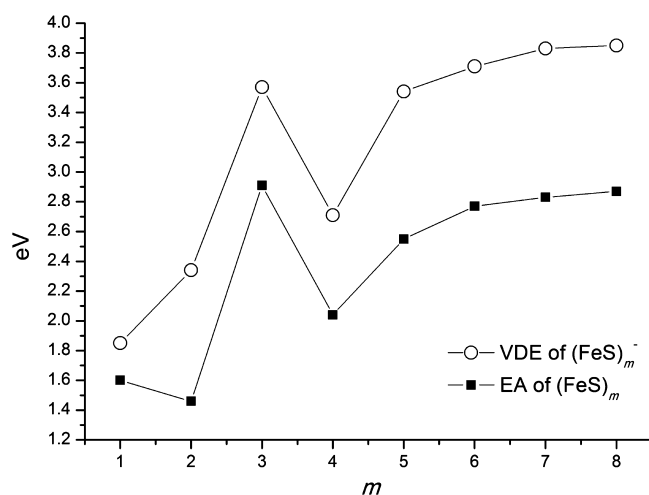


Figure 5. Observed experimental electron binding energies (the first VDEs) of $(\text{FeS})_m^-$ ($m = 1-8$) and adiabatic electron affinities (EA) of $(\text{FeS})_m$ ($m = 1-8$) as a function of number m . The first VDE for FeS^- and EA for FeS are taken from ref 42.

VDEs of $(\text{FeS})_m^-$ ($m = 1-8$) and EAs of $(\text{FeS})_m$ ($m = 1-8$) as a function of number m . The first VDE of FeS^- and EA of FeS are taken from ref 42. Experimental first VDEs of $(\text{FeS})_m^-$ ($m = 1, 2, 4, \text{ and } 5$) clusters increase approximately linearly as a function of cluster size m (slope $[\Delta\text{eV}/\Delta m] \sim 0.4$), while the first VDEs of $(\text{FeS})_m^-$ ($m = 6-8$) clusters do not increase with cluster size (slope $[\Delta\text{eV}/\Delta m] \sim 0$). The cluster $(\text{FeS})_3^-$ is

apparently special in that it has a high first VDE (3.57 eV) close to the value of $(\text{FeS})_m^-$ ($m = 5-8$) clusters.

Synthesis of iron sulfide materials, such as pyrite (FeS_2) thin films and troilite (FeS) nanotubes, has been researched extensively due to their interesting properties for photoelectrochemistry and photovoltaics.^{70,71} Recognizing the importance of the work function for numerous electronic and optoelectronic applications, the work function of pyrite (FeS_2) was indicated to be 5.50 eV.⁷² Unfortunately, the work function of troilite (FeS) is, to the best of our knowledge, not reported.

EA is a measure of the minimum energy required to remove an electron from the ground vibronic state anion, generating the respective neutral species in its vibronic ground state. Wang's group found that for metal cluster anions (such as Fe_n^- , V_n^- , and Ti_n^-) the EAs follow the metallic droplet model, that is, the cluster EAs in general increase with size and eventually approach their respective bulk material work functions.⁷³⁻⁷⁵ To predict the work function of troilite (FeS), we assume the EAs of these $(\text{FeS})_m^-$ ($m = 1-8$) clusters follow the above model. In this work, the EA change trend for $(\text{FeS})_m^-$ ($m = 1-8$) as a function of number m is generally the same as that of the above VDE change trend, as shown in Figure 5. The classical metallic droplet model is usually used to describe the changes of EAs as a function of size.⁷⁶ The metallic droplet model predicts a linear dependence of the EAs on $1/R$ with R as the radius of the cluster. Since R is proportional to the cubic root of the cluster size, the EAs vs $m^{-1/3}$ are plotted in Figure 6. The EAs begin to

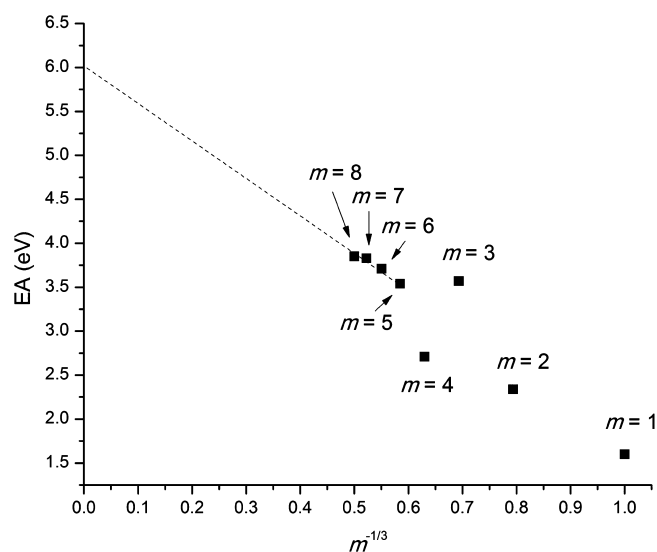


Figure 6. EAs of $(\text{FeS})_m^-$ ($m = 1-8$) as a function of $m^{-1/3}$. The dashed line follows the slope of EA vs $m^{-1/3}$ ($m = 5-8$). The extrapolated value obtained at $m^{-1/3} = 0$ is about 6.0 eV, and this is a possible value for estimation of the work function of the troilite (FeS) solid surface.

follow the above model starting at $(\text{FeS})_5$. Therefore, an extrapolated value of ~ 6.0 eV obtained from Figure 6 is a possible value for estimation of the work function of the troilite (FeS) surface.

To investigate and understand the above first VDE trends, NBOs are calculated for $(\text{FeS})_m^-$ ($m = 1-8$) cluster anions: plots of these distributions for the highest singly occupied molecular orbitals (NBO/HSOMOs) are shown in Figure 7. The NBO/HSOMOs of $(\text{FeS})_{1,2}^-$, with low first VDEs and respective neutral cluster's EAs (as shown in Figure 5), present

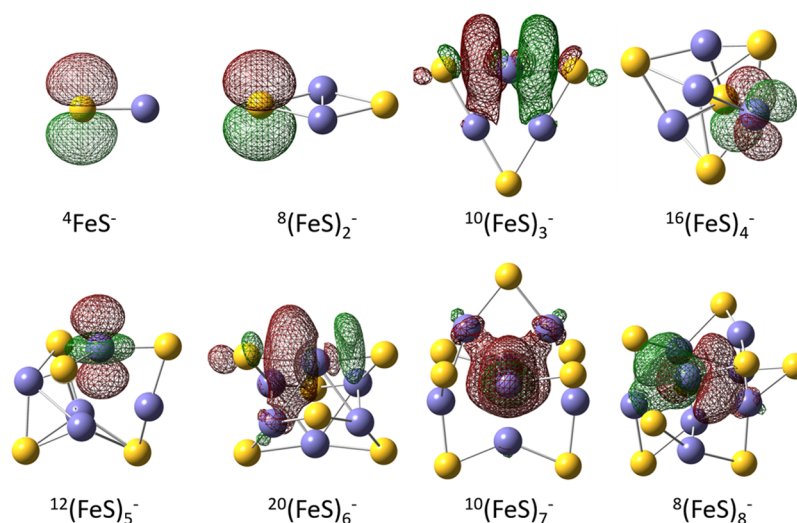


Figure 7. NBO plots showing the highest singly occupied molecular orbital (HSOMO) of $(\text{FeS})_m^-$ ($m = 1-8$) cluster anions. The spin multiplicity (M) is listed as $^M(\text{FeS})_m^-$.

similar electron distributions to those of localized p orbitals on S. clusters $(\text{FeS})_{1,2}$ are found to have high reactivity with CO and H_2 .¹⁹ Interestingly, the distributions of NBO/HSOMO of neutral $(\text{FeS})_{1,2}$ are found to be similar to those of their respective anions. This sulfur p orbital localized NBO/HSOMO is possibly responsible for the low first VDE, EA, and high reactivity of these clusters, associated with its “sulfur radical” likely electronic nature. The first VDEs of $(\text{FeS})_{4,5}^-$ are higher than those of $(\text{FeS})_{1,2}^-$, and the NBO/HSOMOs of $(\text{FeS})_{4,5}^-$ appear as localized d orbitals of Fe. Since the S atom is more electronegative than the iron atom, the Fe atom in these iron sulfur clusters is more positively charged than the sulfur atom. Therefore, electron density should be more difficult to remove from the iron atom than the sulfur atom of these clusters. This is probably responsible for the increase of the first VDE of $(\text{FeS})_{4,5}^-$ compared with those of $(\text{FeS})_{1,2}^-$. On the basis of the first VDE trends as displayed in Figure 5, cluster $(\text{FeS})_3^-$ is a special one, whose first VDE is similar to the larger clusters $(\text{FeS})_{6-8}^-$, and higher than that of the $(\text{FeS})_5^-$ cluster. Figure 7 shows the NBO/HSOMO plots for $(\text{FeS})_{3,6-8}^-$ are also similar, and mainly delocalized as expected for Fe–Fe bonding orbitals. Removing electron density from such a bonding orbital probably requires more energy than from sulfur p or iron d orbitals. In sum, the first VDE trend noted can be related to the different electron distribution properties of NBO/HSOMOs of each cluster anion, $(\text{FeS})_m^-$ ($m = 1-8$); of particular note is the changing nature of their NBO/HSOMO from a p orbital on S, to a d orbital on Fe, to an Fe–Fe bonding orbital. Thus, these evolving NBO representations of the electronic distributions in the $(\text{FeS})_m^-$ ($m = 1-8$) clusters are probably reasonable and correlate and explicate the observed increasing trend for anion cluster first VDEs with cluster size. Canonical HSOMOs of $(\text{FeS})_m^-$ ($m = 1-8$) cluster anions obtained from DFT calculations can also be considered (see Figure S4 in the Supporting Information) to analyze the experimental result; however, the electron distribution properties of these canonical HSOMOs for $(\text{FeS})_m^-$ ($m = 1-8$) cluster anions are undistinguished. Their canonical HSOMO plots are similar, and electron density is localized on all Fe and S atoms. These canonical orbitals do not give the observed trends evidenced through the above NBOs. Therefore, the NBOs are apparently more useful orbitals for

understanding the observed trends of the first VDEs of $(\text{FeS})_m^-$ ($m = 1-8$) cluster anions with cluster size.

CONCLUSIONS

Iron sulfur $(\text{FeS})_m^-$ ($m = 2-8$) cluster anions are studied by PES at 3.492 eV (355 nm) and 4.661 eV (266 nm) photon energies and by DFT calculations. The structural properties, relative energies of different spin states, and first calculated VDEs of different spin states for these $(\text{FeS})_m^-$ ($m = 2-8$) cluster anions are investigated at the BPW91/TZVP level. The most probable structures and ground state spin multiplicities for $(\text{FeS})_m^-$ ($m = 2-8$) clusters are tentatively assigned by comparing their theoretical and experimental first VDE values. Calculated and experimental adiabatic electron affinities of these ground state $(\text{FeS})_m^-$ ($m = 2-8$) neutral clusters are also reported. On the basis of the calculated relative energies for the spin states of each $(\text{FeS})_m^-$ ($m = 2-8$), many spin states lie within 0.5 eV of the ground spin state: this is particularly true for the larger $(\text{FeS})_m^-$ ($m \geq 4$) clusters. Theoretical VDEs of most of these latter low lying spin states for $(\text{FeS})_m^-$ ($m \geq 4$) clusters are in good agreement with their experimental VDE values. Therefore, multiple spin states of each of these iron sulfur cluster anions probably coexist under the experimental conditions. Such available multiple spin states must be considered when evaluating the properties and behavior of these iron sulfur clusters in real chemical and biological systems.

The experimental first VDEs for $(\text{FeS})_m^-$ ($m = 1, 2, 4, 5$) cluster anions are observed to increase with number m from 1.8 to 3.5 eV; the first experimental VDE for $(\text{FeS})_3^-$ (~ 3.6 eV) is an exception to this trend. The first VDEs of $(\text{FeS})_m^-$ ($m = 6-8$) cluster anions are also high (~ 3.8 eV) and are similar. The VDE trends noted can be related to the different properties of the highest singly occupied molecular orbitals (NBO/HSOMOs) of each cluster anion, $(\text{FeS})_m^-$ ($m = 1-8$): the NBO/HSOMOs of $(\text{FeS})_{1,2}^-$ are localized p orbitals of S; the NBO/HSOMOs of $(\text{FeS})_{4,5}^-$ are localized d orbitals of Fe; and the NBO/HSOMOs of $(\text{FeS})_{3,6-8}^-$ are mainly delocalized as Fe–Fe bonding orbitals. The changing nature of the NBO/HSOMO of these $(\text{FeS})_m^-$ ($m = 1-8$) clusters, from a p orbital on S, to a d orbital on Fe, to an Fe–Fe bonding orbital, is

probably responsible for the observed increasing trend for their first VDEs.

■ ASSOCIATED CONTENT

■ Supporting Information

The Supporting Information is available free of charge on the ACS Publications website at DOI: 10.1021/acs.jpca.7b07676.

(1) Optimized geometries in Cartesian coordinates for $(\text{FeS})_8^-$ clusters; (2) brief description of broken symmetry; (3) mass spectra of Fe_mS_n^- cluster anions obtained by different methods; (4) relative energy of $(\text{FeS})_8^-$ clusters with different spin multiplicities; (5) canonical orbital plots showing the highest singly occupied molecular orbital (HSOMO) of $(\text{FeS})_m^-$ ($m = 1-8$) cluster anions; and (6) spin orbit coupling corrected calculational results for $(\text{FeS})_{1,2}^-$ clusters (PDF)

■ AUTHOR INFORMATION

Corresponding Author

*E-mail: erb@colostate.edu.

ORCID

Shi Yin: 0000-0001-7414-4945

Elliot R. Bernstein: 0000-0003-0045-7193

Notes

The authors declare no competing financial interest.

■ ACKNOWLEDGMENTS

This work is supported by a grant from the US Air Force Office of Scientific Research (AFOSR) through Grant FA9550-10-1-0454, the National Science Foundation (NSF) ERC for Extreme Ultraviolet Science and Technology under NSF Award No. 0310717, the Army Research Office (ARO, Grants FA9550-10-1-0454 and W911-NF13-10192), and a DoD DURIP Grant (W911NF-13-1-0192).

■ REFERENCES

- Beinert, H.; Holm, R. H.; Munck, E. Iron-Sulfur Clusters: Nature's Modular, Multipurpose Structures. *Science* **1997**, *277*, 653–659.
- Cammack, R. *Advances in Inorganic Chemistry*; Academic Press: New York, 1992; Vol. 38.
- Nurmaganbetova, M. S.; Baikenov, M. I.; Meiramov, M. G.; Mukhtar, A. A.; Ordabaeva, A. T.; Khрупov, V. A. Catalytic Hydrogenation of Anthracene on Modified Iron Sulfide Catalysts. *Pet. Chem.* **2001**, *41*, 26–29.
- Munck, E.; Bominaar, E. L. Chemistry - Bringing Stability to Highly Reduced Iron-Sulfur Clusters. *Science* **2008**, *321*, 1452–1453.
- Rees, D. C.; Howard, J. B. The Interface between the Biological and Inorganic Worlds: Iron-Sulfur Metalloclusters. *Science* **2003**, *300*, 929–931.
- Bryant, R. D.; Kloeke, F. V.; Laishley, E. J. Regulation of the Periplasmic Fe Hydrogenase by Ferrous Iron in *Desulfovibrio-Vulgaris* (Hildenborough). *Appl. Environ. Microbiol.* **1993**, *59*, 491–495.
- Holm, R. H.; Kennepohl, P.; Solomon, E. I. Structural and Functional Aspects of Metal Sites in Biology. *Chem. Rev.* **1996**, *96*, 2239–2314.
- Jang, S. B.; Seefeldt, L. C.; Peters, J. W. Insights into Nucleotide Signal Transduction in Nitrogenase: Structure of an Iron Protein with Mgadp Bound. *Biochemistry* **2000**, *39*, 14745–14752.
- Einsle, O.; Tezcan, F. A.; Andrade, S. L. A.; Schmid, B.; Yoshida, M.; Howard, J. B.; Rees, D. C. Nitrogenase Mofe-Protein at 1.16 Å Resolution: A Central Ligand in the Femo-Cofactor. *Science* **2002**, *297*, 1696–1700.
- Doukov, T. I.; Iverson, T. M.; Seravalli, J.; Ragsdale, S. W.; Drennan, C. L. A Ni-Fe-Cu Center in a Bifunctional Carbon Monoxide Dehydrogenase/ Acetyl-Coa Synthase. *Science* **2002**, *298*, 567–572.
- Peters, J. W.; Lanzilotta, W. N.; Lemon, B. J.; Seefeldt, L. C. X-Ray Crystal Structure of the Fe-Only Hydrogenase (CpI) from *Clostridium Pasteurianum* to 1.8 Ångstrom Resolution. *Science* **1998**, *282*, 1853–1858.
- Berkovitch, F.; Nicolet, Y.; Wan, J. T.; Jarrett, J. T.; Drennan, C. L. Crystal Structure of Biotin Synthase, an S-Adenosylmethionine-Dependent Radical Enzyme. *Science* **2004**, *303*, 76–79.
- Lukianova, O. A.; David, S. S. A Role for Iron-Sulfur Clusters in DNA Repair. *Curr. Opin. Chem. Biol.* **2005**, *9*, 145–151.
- Kiley, P. J.; Beinert, H. The Role of Fe-S Proteins in Sensing and Regulation in Bacteria. *Curr. Opin. Microbiol.* **2003**, *6*, 181–185.
- Ogino, H.; Inomata, S.; Tobita, H. Abiological Iron-Sulfur Clusters. *Chem. Rev.* **1998**, *98*, 2093–2122.
- Koszinowski, K.; Schröder, D.; Schwarz, H. Formation and Reactivity of Gaseous Iron-Sulfur Clusters. *Eur. J. Inorg. Chem.* **2004**, *2004*, 44–50.
- Koszinowski, K.; Schröder, D.; Schwarz, H.; Liyanage, R.; Armentrout, P. B. Thermochemistry of Small Cationic Iron-Sulfur Clusters. *J. Chem. Phys.* **2002**, *117*, 10039–10056.
- Whetten, R. L.; Cox, D. M.; Trevor, D. J.; Kaldor, A. Free Iron Clusters React Readily with Oxygen and Hydrogen Sulfide, but Are Inert toward Methane. *J. Phys. Chem.* **1985**, *89*, 566–569.
- Yin, S.; Wang, Z. C.; Bernstein, E. R. Formaldehyde and Methanol Formation from Reaction of Carbon Monoxide and Hydrogen on Neutral Fe_3S_2 Clusters in the Gas Phase. *Phys. Chem. Chem. Phys.* **2013**, *15*, 4699–4706.
- Zhai, H.-J.; Kiran, B.; Wang, L.-S. Electronic and Structural Evolution of Monoiron Sulfur Clusters, FeS_n^- and FeS_n ($n = 1-6$), from Anion Photoelectron Spectroscopy. *J. Phys. Chem. A* **2003**, *107*, 2821–2828.
- Nakajima, A.; Hayase, T.; Hayakawa, F.; Kaya, K. Study on Iron-Sulfur Cluster in Gas Phase: Electronic Structure and Reactivity. *Chem. Phys. Lett.* **1997**, *280*, 381–389.
- Zhang, N.; Hayase, T.; Kawamata, H.; Nakao, K.; Nakajima, A.; Kaya, K. Photoelectron Spectroscopy of Iron-Sulfur Cluster Anions. *J. Chem. Phys.* **1996**, *104*, 3413–3419.
- Fu, Y. J.; Yang, X.; Wang, X. B.; Wang, L. S. Probing the Electronic Structure of $[2\text{Fe-2S}]$ Clusters with Three Coordinate Iron Sites by Use of Photoelectron Spectroscopy. *J. Phys. Chem. A* **2005**, *109*, 1815–1820.
- Fu, Y. J.; Laskin, J.; Wang, L. S. Electronic Structure and Fragmentation Properties of $[\text{Fe}_4\text{S}_4(\text{SET})_{4-x}(\text{SSET})_x]^{2-}$. *Int. J. Mass Spectrom.* **2007**, *263*, 260–266.
- Fu, Y. J.; Laskin, J.; Wang, L. S. Collision-Induced Dissociation of $[4\text{Fe-4S}]$ Cubane Cluster Complexes: $\text{Fe}_4\text{S}_4\text{Cl}_{4-x}(\text{SC}_2\text{H}_5)_x^{2-/1-}$ ($x = 0-4$). *Int. J. Mass Spectrom.* **2006**, *255-256*, 102–110.
- Yang, X.; Niu, S. Q.; Ichiye, T.; Wang, L. S. Direct Measurement of the Hydrogen-Bonding Effect on the Intrinsic Redox Potentials of $[4\text{Fe-4S}]$ Cubane Complexes. *J. Am. Chem. Soc.* **2004**, *126*, 15790–15794.
- El Nakat, J.; Fisher, K. J.; Dance, I. G.; Willett, G. D. Gas Phase Metal Chalcogenide Cluster Ions: A New $[\text{Co}_x\text{S}_y]^-$ Series up to $[\text{Co}_{38}\text{S}_{24}]^-$ and Two Iron-Sulfur $[\text{Fe}_x\text{S}_y]^-$ Series. *Inorg. Chem.* **1993**, *32*, 1931–1940.
- Hubner, O.; Sauer, J. The Electronic States of $\text{Fe}_2\text{S}_2^{-/0/+2+}$. *J. Chem. Phys.* **2002**, *116*, 617–628.
- Hubner, O.; Sauer, J. Structure and Thermochemistry of $\text{Fe}_2\text{S}_2^{-/0/+}$ Gas Phase Clusters and Their Fragments. B3LYP Calculations. *Phys. Chem. Chem. Phys.* **2002**, *4*, 5234–5243.
- Ding, L.-P.; Kuang, X.-Y.; Shao, P.; Zhong, M.-M. Evolution of the Structure and Electronic Properties of Neutral and Anion FeS_n^μ ($n = 1-7$, $\mu = 0,-1$) Clusters: A Comprehensive Analysis. *J. Alloys Compd.* **2013**, *573*, 133–141.

- (31) Noodleman, L.; Peng, C. Y.; Case, D. A.; Mouesca, J. M. Orbital Interactions, Electron Delocalization and Spin Coupling in Iron-Sulfur Clusters. *Coord. Chem. Rev.* **1995**, *144*, 199–244.
- (32) Mouesca, J.-M.; Lamotte, B. Iron-Sulfur Clusters and Their Electronic and Magnetic Properties. *Coord. Chem. Rev.* **1998**, *178–180*, 1573–1614.
- (33) Johnson, D. C.; Dean, D. R.; Smith, A. D.; Johnson, M. K. Structure, Function, and Formation of Biological Iron-Sulfur Clusters. *Annu. Rev. Biochem.* **2005**, *74*, 247–281.
- (34) Flint, D.; Emptage, M.; Finnegan, M.; Fu, W.; Johnson, M. The Role and Properties of the Iron-Sulfur Cluster in Escherichia Coli Dihydroxy-Acid Dehydratase. *J. Biol. Chem.* **1993**, *268*, 14732–14742.
- (35) Harvey, J. N. In *Principles and Applications of Density Functional Theory in Inorganic Chemistry I*; Springer: Berlin, 2004; pp 151–184.
- (36) Beinert, H. Recent Developments in the Field of Iron-Sulfur Proteins. *FASEB J.* **1990**, *4*, 2483–2491.
- (37) Brudvig, G. W.; Beck, W. F.; Paula, J. Mechanism of Photosynthetic Water Oxidation. *Annu. Rev. Biophys. Biophys. Chem.* **1989**, *18*, 25–46.
- (38) MITCHELL, P. The Correlation of Chemical and Osmotic Forces in Biochemistry. *J. Biochem.* **1985**, *97*, 1–18.
- (39) Clima, S.; Hendrickx, M. F. Photoelectron Spectra of FeS⁻ Explained by a CASPT2 Ab Initio Study. *Chem. Phys. Lett.* **2007**, *436*, 341–345.
- (40) Yu, Z.; Zhang, N.; Wu, X.; Gao, Z.; Zhu, Q.; Kong, F. The Production and Photodissociation of Iron-Sulfur Cluster Ions. *J. Chem. Phys.* **1993**, *99*, 1765–1770.
- (41) Corderman, R.; Lineberger, W. Negative Ion Spectroscopy. *Annu. Rev. Phys. Chem.* **1979**, *30*, 347–378.
- (42) Yin, S.; Bernstein, E. R. Properties of Iron Sulfide, Hydrosulfide, and Mixed Sulfide/Hydrosulfide Cluster Anions through Photoelectron Spectroscopy and Density Functional Theory Calculations. *J. Chem. Phys.* **2016**, *145*, 154302.
- (43) Zeng, Z.; Bernstein, E. R. Photoelectron Spectroscopy and Density Functional Theory Studies of N-Rich Energetic Materials. *J. Chem. Phys.* **2016**, *145*, 164302.
- (44) Wu, H.; Desai, S. R.; Wang, L.-S. Chemical Bonding between Cu and Oxygen Copper Oxides vs O₂ Complexes: A Study of CuO_x (x = 0–6) Species by Anion Photoelectron Spectroscopy. *J. Phys. Chem. A* **1997**, *101*, 2103–2111.
- (45) Frisch, M. J.; Trucks, G. W.; Schlegel, H. B.; Scuseria, G. E.; Robb, M. A.; Cheeseman, J. R.; Scalmani, G.; Barone, V.; Mennucci, B.; Petersson, G. A.; et al. *Gaussian 09*; Gaussian, Inc.: Wallingford, CT, 2009.
- (46) Perdew, J. P.; Wang, Y. Accurate and Simple Analytic Representation of the Electron-Gas Correlation-Energy. *Phys. Rev. B: Condens. Matter Mater. Phys.* **1992**, *45*, 13244–13249.
- (47) Weigend, F.; Ahlrichs, R. Balanced Basis Sets of Split Valence, Triple Zeta Valence and Quadruple Zeta Valence Quality for H to Rn: Design and Assessment of Accuracy. *Phys. Chem. Chem. Phys.* **2005**, *7*, 3297–3305.
- (48) Santambrogio, G.; Brümmer, M.; Wöste, L.; Döbler, J.; Sierka, M.; Sauer, J.; Meijer, G.; Asmis, K. R. Gas Phase Vibrational Spectroscopy of Mass-Selected Vanadium Oxide Anions. *Phys. Chem. Chem. Phys.* **2008**, *10*, 3992–4005.
- (49) Beltrán, M. R.; Zamudio, F. B.; Chauhan, V.; Sen, P.; Wang, H.; Ko, Y. J.; Bowen, K. Ab Initio and Anion Photoelectron Studies of Rh_n (n = 1–9) Clusters. *Eur. Phys. J. D* **2013**, *67*, 63.
- (50) Vyboishchikov, S. F.; Sauer, J. Gas-Phase Vanadium Oxide Anions: Structure and Detachment Energies from Density Functional Calculations. *J. Phys. Chem. A* **2000**, *104*, 10913–10922.
- (51) Asmis, K. R.; Santambrogio, G.; Brümmer, M.; Sauer, J. Polyhedral Vanadium Oxide Cages: Infrared Spectra of Cluster Anions and Size-Induced D Electron Localization. *Angew. Chem., Int. Ed.* **2005**, *44*, 3122–3125.
- (52) Rassolov, V. A.; Pople, J. A.; Ratner, M. A.; Windus, T. L. 6-31G* Basis Set for Atoms K through Zn. *J. Chem. Phys.* **1998**, *109*, 1223–1229.
- (53) Krishnan, R.; Binkley, J. S.; Seeger, R.; Pople, J. A. Self-Consistent Molecular Orbital Methods. XX. A Basis Set for Correlated Wave Functions. *J. Chem. Phys.* **1980**, *72*, 650–654.
- (54) Hehre, W. J.; Ditchfield, R.; Pople, J. A. Self-Consistent Molecular Orbital Methods. Xii. Further Extensions of Gaussian Type Basis Sets for Use in Molecular Orbital Studies of Organic Molecules. *J. Chem. Phys.* **1972**, *56*, 2257–2261.
- (55) Dunning, T. H. Gaussian Basis Sets for Use in Correlated Molecular Calculations. I. The Atoms Boron through Neon and Hydrogen. *J. Chem. Phys.* **1989**, *90*, 1007–1023.
- (56) Casida, M. E.; Jamorski, C.; Casida, K. C.; Salahub, D. R. Molecular Excitation Energies to High-Lying Bound States from Time-Dependent Density-Functional Response Theory: Characterization and Correction of the Time-Dependent Local Density Approximation Ionization Threshold. *J. Chem. Phys.* **1998**, *108*, 4439–4449.
- (57) Cederbaum, L. One-Body Green's Function for Atoms and Molecules: Theory and Application. *J. Phys. B: At. Mol. Phys.* **1975**, *8*, 290.
- (58) Hunt, P. A.; Kirchner, B.; Welton, T. Characterising the Electronic Structure of Ionic Liquids: An Examination of the 1-Butyl-3-Methylimidazolium Chloride Ion Pair. *Chem. - Eur. J.* **2006**, *12*, 6762–6775.
- (59) Noodleman, L.; Norman, J. G., Jr; Osborne, J. H.; Aizman, A.; Case, D. A. Models for Ferredoxins: Electronic Structures of Iron-Sulfur Clusters with One, Two, and Four Iron Atoms. *J. Am. Chem. Soc.* **1985**, *107*, 3418–3426.
- (60) Anderson, R. E.; Dunham, W. R.; Sands, R. H.; Bearden, A. J.; Crespi, H. L. On the Nature of the Iron Sulfur Cluster in a Deuterated Algal Ferredoxin. *Biochim. Biophys. Acta, Bioenerg.* **1975**, *408*, 306–318.
- (61) Li, Y.-N.; Wang, S.; Wang, T.; Gao, R.; Geng, C.-Y.; Li, Y.-W.; Wang, J.; Jiao, H. Energies and Spin States of FeS^{0/-}, FeS₂^{0/-}, Fe₂S₂^{0/-}, Fe₃S₄^{0/-}, and Fe₄S₄^{0/-} Clusters. *ChemPhysChem* **2013**, *14*, 1182–1189.
- (62) Ding, L.-P.; Kuang, X.-Y.; Shao, P.; Zhong, M.-M. Probing the Structural, Electronic and Magnetic Properties of Multicenter Fe₂S₂^{0/-}, Fe₃S₄^{0/-} and Fe₄S₄^{0/-} Clusters. *J. Mol. Model.* **2013**, *19*, 1527–1536.
- (63) Becke, A. D. Density-Functional Thermochemistry 3. The Role of Exact Exchange. *J. Chem. Phys.* **1993**, *98*, 5648–5652.
- (64) Lee, C. T.; Yang, W. T.; Parr, R. G. Development of the Colle-Salvetti Correlation-Energy Formula into a Functional of the Electron-Density. *Phys. Rev. B: Condens. Matter Mater. Phys.* **1988**, *37*, 785–789.
- (65) Becke, A. D. Density-Functional Exchange-Energy Approximation with Correct Asymptotic Behavior. *Phys. Rev. A: At, Mol, Opt. Phys.* **1988**, *38*, 3098–3100.
- (66) Perdew, J. P.; Burke, K.; Wang, Y. Generalized Gradient Approximation for the Exchange-Correlation Hole of a Many-Electron System. *Phys. Rev. B: Condens. Matter Mater. Phys.* **1996**, *54*, 16533–16539.
- (67) Austin, A.; Petersson, G. A.; Frisch, M. J.; Dobek, F. J.; Scalmani, G.; Throssell, K. A Density Functional with Spherical Atom Dispersion Terms. *J. Chem. Theory Comput.* **2012**, *8*, 4989–5007.
- (68) Werner, H.-J.; Knowles, P. J.; Knizia, G.; Manby, F. R.; Schütz, M. Molpro: A General-Purpose Quantum Chemistry Program Package. *Wiley Interdiscip. Rev. Comput. Mol. Sci.* **2012**, *2*, 242–253.
- (69) Hübner, O.; Sauer, J. The Electronic States of Fe₂S₂^{-0/+2+}. *J. Chem. Phys.* **2002**, *116*, 617–628.
- (70) Cummins, D. R.; Russell, H. B.; Jasinski, J. B.; Menon, M.; Sunkara, M. K. Iron Sulfide (FeS) Nanotubes Using Sulfurization of Hematite Nanowires. *Nano Lett.* **2013**, *13*, 2423–2430.
- (71) Bhandari, K. P.; Roland, P. J.; Kinner, T.; Cao, Y.; Choi, H.; Jeong, S.; Ellingson, R. J. Analysis and Characterization of Iron Pyrite Nanocrystals and Nanocrystalline Thin Films Derived from Bromide Anion Synthesis. *J. Mater. Chem. A* **2015**, *3*, 6853–6861.
- (72) Trigwell, S.; Mazumder, M. K.; Pellissier, R. Tribocharging in Electrostatic Beneficiation of Coal: Effects of Surface Composition on Work Function as Measured by X-Ray Photoelectron Spectroscopy and Ultraviolet Photoelectron Spectroscopy in Air. *J. Vac. Sci. Technol., A* **2001**, *19*, 1454–1459.

(73) Wang, L.-S.; Li, X.; Zhang, H.-F. Probing the Electronic Structure of Iron Clusters Using Photoelectron Spectroscopy. *Chem. Phys.* **2000**, *262*, 53–63.

(74) Liu, S.-R.; Zhai, H.-J.; Castro, M.; Wang, L.-S. Photoelectron Spectroscopy of Ti_n^- Clusters ($n = 1-130$). *J. Chem. Phys.* **2003**, *118*, 2108–2115.

(75) Wu, H.; Desai, S. R.; Wang, L.-S. Evolution of the Electronic Structure of Small Vanadium Clusters from Molecular to Bulklike. *Phys. Rev. Lett.* **1996**, *77*, 2436.

(76) Wood, D. M. Classical Size Dependence of the Work Function of Small Metallic Spheres. *Phys. Rev. Lett.* **1981**, *46*, 749.